High-Mobility Few-Layer Graphene Field Effect Transistors Fabricated on Epitaxial Ferroelectric Gate Oxides

X. Hong[1], A. Posadas[2], K. Zou[1], C. H. Ahn[2] and J. Zhu[1,*]

[1]Department of Physics, The Pennsylvania State University, University Park, PA 16802

[2]Department of Applied Physics, Yale University, New Haven, CT 06520

Online Supplementary Information Content:

1. Characterizations of $Pb(Zr_{0.2}Ti_{0.8})O_3$ (PZT) films.
2. Substrate preparation before the exfoliation of graphene.
3. The band structure of FLG.
4. Dielectric constant measurements of PZT.
5. $\rho(V_g)$ and $R_H(V_g)$ fitting inside the band overlap regime.
6. The deformation potential of longitudinal acoustic (LA) phonons in graphene.
7. Resistivity and Hall measurements of a SiO_2-gated FLG.

1. Characterizations of $Pb(Zr_{0.2}Ti_{0.8})O_3$ films

The crystalline quality of the PZT thin films is characterized with x-ray diffraction (XRD). Figure S1 shows the θ-2θ measurement of a typical 300 nm $Pb(Zr,Ti)O_3$ (PZT) film grown epitaxially on $SrTiO_3$ (STO) substrate. Only 00*n* (*n* =1, 2, etc.) peaks for PZT and STO are detected, showing a *c*-axis oriented film growth, with the polarization *P* pointing normal to the surface (characterized with piezoresponse force microscopy, see below). The *c*-axis lattice constant is ~4.15 Å, consistent with the value of a partially relaxed film. The rocking curve of the 001 peak has a full-width-half-maximum of 0.04°, close to the instrumental resolution, reflecting very high crystallinity.

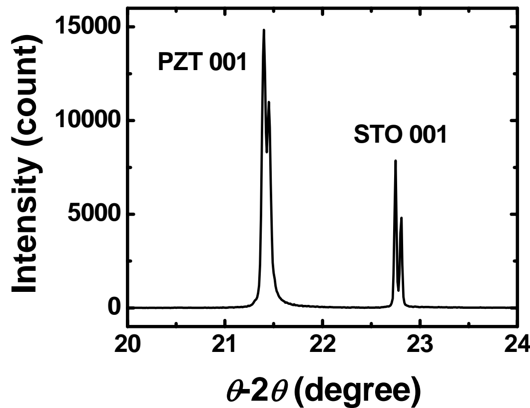

Fig. S1 X-ray θ-2θ measurement of a 300 nm PZT film grown on a $SrTiO_3$ substrate. The double-peak feature is due to the $k_{\alpha 1}$ and $k_{\alpha 2}$ x-rays.

We have chosen film thickness of d = 300 and 400 nm to enhance the optical visibility of graphene through modeling described in Ref. [1]. AC voltages and voltage pulses of different polarity and magnitude are applied to the AFM tip scanning in contact with the PZT surface to perform piezoresponse force microscopy (PFM) [2]. Negative voltage pulses > 8 V are needed to switch the polarization of 400 nm as-grown films. We conclude that *P* uniformly points into the surface, as expected from the growth procedure. The direction of *P* remained unchanged throughout the current study.

2. Substrate preparation before the exfoliation of graphene

Prior to graphene exfoliation, PZT and SiO_2 substrates are sonicated in acetone for 20 minutes followed by an IPA rinse (1 min) and drying under a stream of dry N_2 gas. They are subsequently baked at 120°C for 5 minutes before the exfoliation of graphene.

3. The band structure of FLG

We employ a simply two-band model to estimate the band overlap energy $\delta\varepsilon$ and the densities of electrons and holes in the two-carrier regime near the charge neutrality point of our device, using band parameters determined by Novoselov *et al.* for FLG in Ref. [3] and supporting materials. Measurements there indicate a single electron band with an effective mass $m^*_e = 0.06m_0$ and two hole bands with a heavy hole mass $m^h_h = 0.1m_0$ and a light hole mass $m^l_h = 0.03m_0$. Note these effective mass values are close to those found in bulk graphite: $m^*_e = (0.056\pm0.003)\ m_0$ and $m^*_h = (0.084\pm0.005)\ m_0$ as well [4]. Without knowing the exact offset between the two hole bands, we simplify the estimate by ignoring the light holes, which likely account for less than 25% of the hole population due to the mass ratio. The densities of states of electrons and holes are then given by $\frac{2m^*_{e,h}}{\pi\hbar^2}$, where we have included the 4-fold degeneracy due to valley and spin [3].

The density of electrons and holes in the band overlap regime of the FLG is calculated as follows:

$$n_{e,h} = n^0_{e,h} \pm \frac{\alpha V_g m^*_{e,h}}{(m^*_e + m^*_h)} \qquad \text{(“+” for electron and “–” for hole)} \qquad \text{(S1)},$$

where $n^0_{e,h}$ represents the electron/hole density at the charge neutrality point. At the threshold voltage $V^T_g = 1.1$ V (Fig. 2(b)) where the hole band is completely filled, $n_e = 1.5\text{x}10^{12}/\text{cm}^2$ and $n_h = 0$. Using Eq. S1, we estimate that $n^0_e = n^0_h \sim 9\text{x}10^{11}/\text{cm}^2$ at the charge neutrality point. This translates into a band overlap of $\delta\varepsilon \sim 30$ meV between the electron and hole bands. Alternatively, we determine $\delta\varepsilon$ by fitting $\rho(T)$ at the charge neutrality point to the thermal excitation model described in Ref. [3] and obtain $\delta\varepsilon \sim 27$

meV. The good agreement between these two methods and with theory [5] gave us confidence in these estimates. However we emphasize that the central results of our paper are derived from the electron-only regime ($V_g > V^T_g$) and do not rely on an accurate knowledge of the band structure in the two-carrier regime.

4. Dielectric constant measurements of PZT

We deduce the dielectric constant κ of PZT substrate by Hall and low-frequency capacitance measurements independently. Figure S2 shows hole densities extracted from Hall measurements as a function of the backgate voltage V_g in three different devices placed on the same PZT substrate, including the device shown in Fig. 2. We determine the charge injection rate α = (1.35±0.05)x10^{12} cm^{-2}/V_g(V) using Eq. (2) in the single carrier (hole) regime, and calculate $\kappa \approx 100$ using a parallel-plate capacitor model.

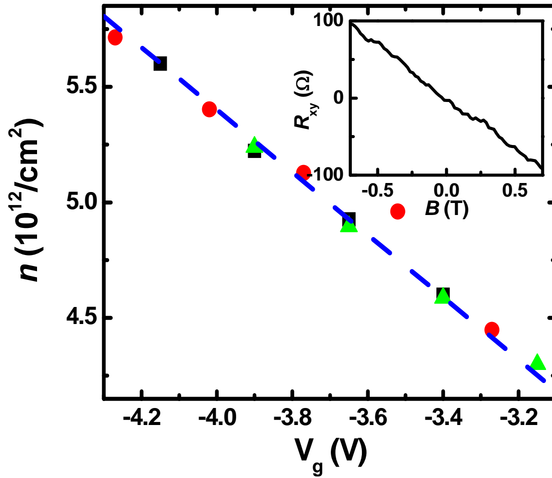

Fig. S2 Hole density n vs. backgate voltage V_g taken on three devices (squares, circles and triangles) on the same PZT substrate. The fit (blue dashed line) corresponds to a charge injection rate of 1.35x10^{12} cm^{-2}/V. V_g is shifted to align the charge neutrality point at V_g = 0 V as described in the text. Inset: Hall resistance R_{xy} vs. perpendicular magnetic field for n = 4.6x10^{12}/cm^2.

We also determine κ directly through low-frequency (20-1000 Hz) capacitance measurements. Capacitors with varying areas are measured to eliminate the effect of parasitic capacitances. We calculate the area of a capacitor from the mask design and estimate $\kappa \approx 120$ from these measurements.

5. ρ (V_g) fitting inside the band overlap regime

We fit our low-T ρ (V_g) data to Eqs. (1) and (3) within the band overlap regime, using effective masses of $m^*_e = 0.06m_0$ and $m^*_h = 0.1m_0$. A different set of mass values may lead to a different band overlap $\delta\varepsilon$ and affects the value of the exponent β in Eq. (3). For example, $\delta\varepsilon \sim$ 32 meV and $\beta \sim$ 1.0, or $\delta\varepsilon \sim$ 27 meV and $\beta \sim$ 0.8 can fit the same data equally well as the values used in the text ($\delta\varepsilon \sim$ 30 meV and $\beta \sim$ 0.9). Beyond this energy range of $\delta\varepsilon$ (27-32 meV), a power-law n-dependence of mobility no longer describes the data well. The above analysis shows that although the precise value of β depends on $\delta\varepsilon$ and hence the detailed understanding of the band structure of FLG, the power-law n-dependence seems to be robust.

This n-dependence of mobility is also supported by the measurements of the Hall coefficient R_H. Within the band overlap regime, R_H exhibits the characteristics of a two-carrier system described by Eq. S2:

$$R_H = \frac{n_h\mu_h^2 - n_e\mu_e^2}{e(n_h\mu_h + n_e\mu_e)^2} \quad \text{(S2).}$$

At high $|V_g|$, the system becomes a purely electron or hole gas and R_H reads:

$$R_H = \frac{1}{en_{e,h}} = \frac{1}{e\alpha(V_g - V_g^0)} \quad \text{(S3),}$$

Where for PZT-gated samples $\alpha = 1.35\text{x}10^{12}$ cm^{-2}/V and V^0_g is offset to 0 V. Figure S3 plots R_H vs. V_g of the FLG shown in Fig. 2, together with three fitting curves. R_H calculated using Eq. (S2) with $n_{e,h}$ given by Eq. (S1) and $\mu_{e,h}$ given by Eq. (3) with $\beta = 0.9$ and r = 0.6 (red) produce an excellent agreement with the data. Calculations based on a

constant mobility $\mu_h = \mu_e$ = const. (green), or an n-dependent but symmetric electron and hole mobility $\mu_h = \mu_e \sim n^{0.9}$ (blue) clearly do not fit the data.

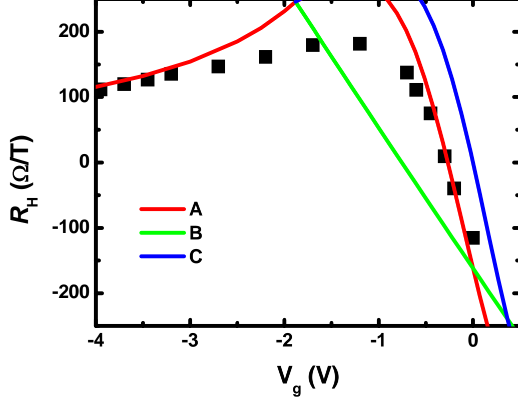

Fig. S3 Hall coefficient R_H vs. V_g at 10 K with three calculated curves. Curve A (red): $\mu_{e,h} \sim n_{e,h}^{0.9}$, $\mu_h/\mu_e = 0.6$ (Eq. 3 of text). Curve B (green): $\mu_h = \mu_e$ = const. Curve C (blue): $\mu_h = \mu_e \sim n^{0.9}$. The charge injection rate $\alpha = 1.35\text{x}10^{12}\text{cm}^{-2}/\text{V}$.

6. The deformation potential of LA phonons in graphene

In Eq. (4), we assume an unscreened deformation potential D for LA phonons. Studies in GaAs show that neglecting the dielectric screening may result in an underestimate of the deformation potential [6]. The detailed T-dependence in the BG regime from a sample of yet higher mobility is required to determine the effect of screening. This analysis is beyond the scope of the present paper.

7. Resistivity and Hall measurements of a SiO_2-gated FLG

To compare the performance of PZT and SiO_2 substrates, we fabricate a FLG-FET of the same thickness (2.4 nm) on 300 nm SiO_2 following identical preparation steps. Figure S4 shows $\rho(V_g)$ of the SiO_2-gated FLG at selected temperatures. The charge neutrality point occurs at V^0_g = - 15.5 V due to unintentional chemical doping. We find the charge injection rate of the backgate to be $\alpha = 7.0\text{x}10^{10}$ cm^{-2}/V, in excellent agreement with calculations and experimental values from other graphene FETs made from the same set

of wafers. We determine $\mu(T)$ using Eq. (2) at electron density $n = 2.4\text{x}10^{12}$ cm^{-2} (V_g = 19 V). The results are plotted in Fig. 4 as open triangles. The mobility μ is approximately 14,000 cm^2/Vs and shows a very weak T-dependence. These findings are in good agreement with what has been reported in the literature [3].

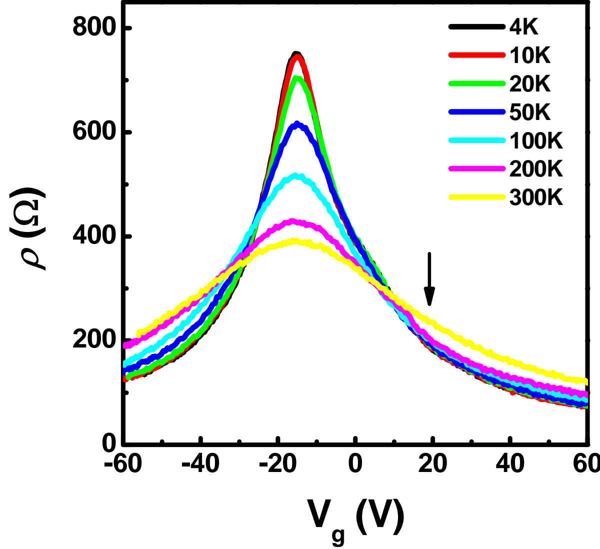

Fig. S4 $\rho(V_g)$ of the SiO_2-gated FLG (2.4 nm) at selected temperatures 4 K < T < 300 K. The charge neutrality point V^0_g = - 15.5 V. The arrow marks V_g = 19 V corresponding to n = 2.4x10^{12} cm^{-2}, where we determine the mobility plotted in Fig. 4.

Figure S5 shows R_H vs. V_g in this FLG. The band overlap, electron-only and hole-only regimes are all clearly visible. Red solid lines are calculated from Eq. (S3) using α =7.0x10^{10} cm^{-2}/V and V^0_g = - 15.5 V. The transition voltage to the electron-only regime (~ 2 V) is in good agreement with that of the PZT-gated FLG, indicated by an arrow.

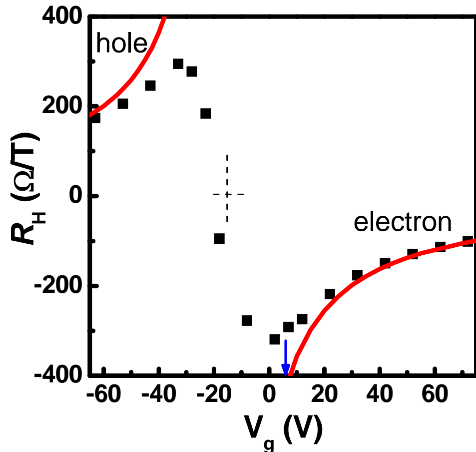

Fig. S5 Hall coefficient R_H vs. V_g (T = 4 K) of the SiO_2-gated FLG. Red solid lines are calculated using Eq. S3 and correspond to electron- and hole-only regime, respectively. The blue arrow indicates the equivalent voltage of the band edge observed in the PZT-gated FLG of the same thickness. The cross marks (-15.5V, 0 Ω/T).

References:

[1] P. Blake *et al.*, Applied Physics Letters **91**, 063124 (2007).
[2] C. H. Ahn, K. M. Rabe, and J.-M. Triscone, Science **303**, 488 (2004).
[3] K. S. Novoselov *et al.*, Science **306**, 666 (2004).
[4] M. S. Dresselhaus, and G. Dresselhaus, Advances in Physics **51**, 1 (2002).
[5] B. Partoens, and F. M. Peeters, Physical Review B **74**, 075404 (2006).
[6] H. L. Stormer *et al.*, Physical Review B **41**, 1278 (1990).